

Advancing Characterization of Materials by Multimodal 4D-STEM Analytical Methods

April 26, 11:00am - 12:00pm EDT

Development and production of new materials and semiconductor devices require morphological, structural, and chemical characterization at the nanoscale level to understand their chemico-physical properties and optimize their production process. Besides traditional electron microscopy imaging and compositional analysis techniques, 4D-STEM methods provide additional structural information about the local internal organization of atoms and molecules at each position of an acquired STEM map.

Watch this session during the WAS Virtual Conference:



Dr. Daniel Nemecek



Dr. Tingting Yang

[Register Now](#)

Production of fungal chitosan and fabrication of fungal chitosan/polycaprolactone electrospun nanofibers for tissue engineering

Sevim Feyza Erdoğan¹ | Özlem Erdal Altıntaş² | Sefa ÇELİK³

¹Department of Basic Pharmaceutical Sciences, Faculty of Pharmacy, Afyonkarahisar Health Sciences University, Afyonkarahisar, Turkey

²Department of Medical Services and Techniques, Şuhut Vocational School of Health Services, Afyonkarahisar Health Sciences University, Afyonkarahisar, Turkey

³Department of Medical Biochemistry, Faculty of Medicine, Afyonkarahisar Health Sciences University, Afyonkarahisar, Turkey

Correspondence

Sevim Feyza Erdoğan, Department of Basic Pharmaceutical Sciences, Faculty of Pharmacy, Afyonkarahisar Health Sciences University, Afyonkarahisar, 03030, Turkey.
Email: feyzakus@gmail.com and feyza.erdogmus@afsu.edu.tr

Funding information

This study was supported by a project of the Afyonkarahisar Health Sciences University Research Foundation, Project No. 19. TEMATİK. 005.

Review Editor: Mingying Yang

Abstract

The present study investigated that chitosan production of *Rhizopus oryzae* NRRL 1526 and *Aspergillus niger* ATCC 16404. Fungal chitosans were characterized by scanning electron microscopy (SEM)-energy dispersive X-ray analysis, Fourier transform infrared spectroscopy (FTIR), differential scanning calorimeter and deacetylation degrees of fungal chitosans were determined. The percentage yield of Ro-chitosan and An-chitosan were determined as 18.6% and 12.5%, respectively. According to percentage of chitosan yield and the results of the characterization studies, chitosan that obtained from *Rhizopus oryzae* NRRL 1526 was selected for subsequent studies. Cytotoxicity of chitosan obtained from *Rhizopus oryzae* NRRL 1526 was determined by MTT assay on human dermal fibroblast cell line. According to results of the cytotoxicity test fungal chitosan was nontoxic on cells. The high cell viability was observed 375 µg/mL concentration at 24th, 48th h periods and at the 187.5 µg/ml 72nd h periods on cells. The fungal chitosan obtained from *Rhizopus oryzae* NRRL 1526 was used to fabrication of electrospun nanofibers. Fungal chitosan based polymer solutions were prepared by adding different substances and different electrostatic spinning parameters were used to obtain most suitable nanofiber structure. Characterization studies of nanofibers were carried out by SEM, FTIR and X-ray diffraction. The most suitable nanofiber structure was determined as F4 formula. The nanofiber structure was evaluated to be thin, bead-free, uniform, flexible and easily remove from surface and taking the shape of the area. After the characterization analysis of fungal chitosan it was determined that the chitosan, which obtained from *Rhizopus oryzae* NRRL 1526 is actually chitosan polymer and this polymer is usable for pharmaceutical areas and biotechnological applications. The electrospun nanofiber that blends fungal chitosan and PCL polymers were fabricated successfully and that it can be used as fabrication wound dressing models.

Research Highlights

Extraction of chitosan from *Rhizopus oryzae* NRRL 1526 and *Aspergillus niger* ATCC 16404 and characterization scanning electron microscopy-energy dispersive X-ray

This is an open access article under the terms of the [Creative Commons Attribution-NonCommercial-NoDerivs](https://creativecommons.org/licenses/by-nc-nd/4.0/) License, which permits use and distribution in any medium, provided the original work is properly cited, the use is non-commercial and no modifications or adaptations are made.

© 2023 The Authors. *Microscopy Research and Technique* published by Wiley Periodicals LLC.

analysis, Fourier transform infrared spectroscopy, differential scanning calorimeter. Fabrication and characterization of the fungal chitosan/PCL electrospun nanofibers.

KEYWORDS

Aspergillus Niger ATCC 16404, chitosan, nanofiber, *Rhizopus oryzae* NRRL 1526

1 | INTRODUCTION

Electrospinning is a simple, effective, versatile and most widely used technique that allows the production of nanosized fibers from different polymer depending on the property of polymer and processing conditions (Huang et al., 2003; Ramakrishna et al., 2005). This technique was first discovered in the seventeenth century by William Gilbert (Tucker et al., 2012). In this process, polymer solution or melt, fed from the tip of a capillary to a collector, is exposed to an electric field. Once surface tension of the solution or melt droplet at the tip is overcome by electric field and coulombic forces, charged droplet generates the Taylor cone. As the critical voltage is exceeded an electrified emerges from the tip of the Taylor cone. During the traveling to the collector, stretching and elongation take place and finally nanofibers are formed as the solvent evaporates or melt cools down (Tripatanasuwan et al., 2007). Electrospun biopolymer nanofibers have potential uses as scaffolds, wound dressings and drug release systems due to their resemblance to natural extra cellular matrix, high surface area to volume ratio, increased flexibility in surface functionalities, improved mechanical performances, and smaller porosities (Schiffman & Schauer, 2007; Subbiah et al., 2005). The wide range of polymers are capable of being electrospun nanofibers from pure or blended of natural polymers such as collagen, fibroin, silk, carboxymethyl cellulose, hyaluronic acid and chitosan and synthetic polymers as polyvinylalcohol, polycaprolactone, polyethyleneoxide (Chen et al., 2017; Fathollahipour et al., 2015; Kamoun & Kenawy, 2017; Majd et al., 2016; Nemati et al., 2019; Venugopal et al., 2010). Biopolymers are biocompatible, biodegradable, non-toxic and similar to extracellular matrices, by contrast synthetic polymers do not have these features. However, synthetic polymers provide great applicability by chemical or physical modifications, as well as excellent processability (Li et al., 2006). Nevertheless, single component biopolymer is generally insufficient for good physical and biochemical fiber specifications. To overcome these limitations, recent effort has been given to takes advantage of the physical properties of the synthetic polymers and the bioactivity of the biopolymers while minimizing disadvantages of both combined for the preparation of electrospun fibers (Kweon et al., 2001; Lin et al., 2013; Shao et al., 2016).

Chitosan is a natural and recyclable biopolymer obtained by deacetylation of chitin (Abeer Mohammed, 2018). Chitin is generally found in nature, has a structure of antiparallel chains and is found in crabs, shrimps, seaweeds, protozoa, cetaceans, mollusks, arthropods, bacteria, fungi, insects and some plants (Ifuku, 2014). Fungi have significant quantity of chitin in their cell walls, and upon the extraction of chitosan from these cells (Kucera, 2004; Nwe et al., 2002). Many researches

have been carried out for the production of chitin and chitosan from fungi (Akila, 2014; Muslim et al., 2018; Sebastian et al., 2019; Wu et al., 2005). Fungi have several advantages in chitosan production, like as suitability for many biomedical applications, low molecular weights, controllability of molecular weight, and deacetylation degree by changing fermentation conditions, high availability of fungal biomass (Bordes & Averous, 2009). Chitosan is a vulnerable polymer and has been used in several areas, for instance cosmetics, pharmacology and medicine, food additives and agriculture biotechnological approaches, agricultural production (Li et al., 2011; No et al., 2007). Also, chitin and chitosan possess many beneficially biological properties such as biocompatibility, biodegradability, hemostatic activity, wound healing, antimicrobial property, low toxicity, that make them notable to biomedical applications (Jayakumar et al., 2010; Tajdini et al., 2010).

The aim of present study is the production and characterization of fungal chitosan, a biopolymer with the desired properties for nanofiber production, obtained from fungal sources. It has been observed that chitosan of fungal origin has been obtained in previous studies carried, but no study has been devoted to production on nanofiber fabrication. In present study, the electrospinning technique was used to produce polymeric scaffolds from a biopolymer derived from fungi with biocompatible polycaprolactone (PCL) polymer, which was chosen as a carrier for its favorable surface properties to produce a novel material nanofiber with better characterization for biomedical applications.

2 | MATERIALS AND METHODS

2.1 | Fungal strain and production biomass

Rhizopus oryzae NRRL 1526 and *Aspergillus niger* ATCC 16404 that have high chitosan production ability as a result of literature review were used in present study for obtained fungal derived chitosan (Abeer Mohammed, 2018; Sebastian et al., 2019). Potato dextrose broth (PDB) and potato dextrose agar (PDA) medium (Merck, Darmstadt, Germany) were used for the cultivation, growing and maintenance of the fungal culture. Fungal cultivation and production biomass were performed according to Pochanavanich and Suntornsuk (2002) method. First, 1 ml spore suspension (10^7 spores mL^{-1}) was inoculated into 100 ml PDB in a 250 ml erlenmeyer flask and incubated at 30°C, 180 rpm, for 6 days. After the incubation period fungal mycelia were filtrated with Whatman filter paper No. 4 and washed twice by distilled water then the biomass pellets were dried at 60°C to constant weight in oven. After the dried samples were ground, yield calculations were performed and stored in the refrigerator at +4°C to be used in other stages.

2.2 | Chitosan extraction

Chitosan extraction was carried out by a modified method of Klee-kayai and Suntornsuk (2010). In this method, biomasses were suspended with 1 M NaOH (1:30, w/v) and autoclaved at 121°C for 15 min. Alkali insoluble fractions were separated by centrifugation at 15,000 g for 25 min and these fractions were washed by distilled water and re-centrifuged to a neutral pH. The residues were further extracted with 2% (v/v) acetic acid (1:40, w/v) at 95°C for 8 h. The extracted slurry was centrifuged and the acid insoluble fractions were discarded. The pH of supernatant was adjusted to 9–10 with 2 N NaOH, and then chitosan was obtained by precipitation through centrifugation and washed with distilled water, 95% (v/v) ethanol (1:20, w/v) and acetone (1:20, w/v), respectively. The fungal chitosans were dried at 50°C for 24 h and weighed to calculate chitosan yields.

2.3 | Characterization of fungal chitosan

The morphology and elemental composition of the chitosan that obtained from *R. oryzae* NRRL 1526 (Ro-chitosan), chitosan that obtained from *A. niger* ATCC 16404 (An-chitosan), commercial chitosan were analyzed by scanning electron microscopy-energy dispersive X-ray analysis (SEM–EDX). The samples were sputtercoated with gold for 30 s at 100 mA prior to imaging with a LEO 1430 VP SEM (Carl Zeiss AG, Jena, Germany) at an accelerating voltage of 20 kV. EDX analysis is a method that used in the elemental analysis of materials. It is a module connected to a scanning electron microscope.

The characterization of Ro-chitosan, An-chitosan and commercial chitosan were performed by using Perkin Elmer Spectrum Two fourier transform infrared spectroscopy (FTIR) recorded in KBr pellet with a resolution of 4 cm⁻¹ and the wavelength ranging from 400 to 4,000 cm⁻¹ at room temperature. The amide I band at 1655 cm⁻¹ and the hydroxyl group absorption band at 3450 cm⁻¹ were used as internal reference (Sebastian et al., 2019). The degree of deacetylation (% DD) was calculated by measuring the absorbance ratio of A₁₆₅₅ and A₃₄₅₀ by the following equation [30] Commercial chitosan (Sigma-Aldrich, Germany) were used for the comparison study.

$$\%DD = 100 - (A_{1655} \div A_{3450}) \times 100/1.33$$

Also thermal stability of Ro-chitosan, An-chitosan and commercial chitosan were examined by using differential scanning calorimeter (Perkin Elmer DSC-8000) under a nitrogen at the at a flow rate of 5 ml/min and the heating rate of 50°C/min from room temperature to 300°C (Jana et al., 2014).

2.4 | Cytotoxicity of fungal chitosan

Cytotoxicity of Ro-chitosan that produced high chitosan yield was determined by MTT assay on Human dermal fibroblast cell line (HDFa) (Kumar et al., 2018). First, cells at the 70%–80% confluency

were trypsinized and seeded on to a 96-well plate at the cell/well density of 1 × 10⁴. The HDFa cells (ATCC, PCS-201-012) were cultured using Dulbecco's modified Eagle's medium (DMEM), 10% fetal bovine serum and 1% penicillin–streptomycin solution (Sigma-Aldrich, Germany). HDFa cells were first seeded in 96 well plates at a density of 2 × 10⁴ cells per well, treated with different concentrations of fractions (46.87–1500 µg/ml), and incubated at 37°C with 5% of CO₂ and 95% of humidity for 24, 48 and 72 h. Then MTT 1-(4,5-dimethylthiazol-2-yl)-3,5-diphenylformazan, thiazolyl blue formazan (Sigma-Aldrich, Germany) reagent was added onto wells and incubated at 37°C for 2 h. After incubation, MTT reagent was removed from the cells, DMSO was added to each well, and the plate was shaken at low speed for 5 min at room temperature. Absorbance values were measured with Gen5 Biotek Microplate Reader (BioTek, Epoch, ABD) at wavelength of 570 nm and cell viability was calculated. Untreated cells (cells on wells without any sample but DMEM media) were used as a control and considered as 100% viable. All experiments were performed in triplicate, and statistical analysis of in vitro test data was performed via GraphPad Prism 9 with One-Way ANOVA and Tukey's multiple comparisons tests.

2.5 | Fabrication of electrospun fungal chitosan based nanofiber

The Ro-chitosan was used to fabrication of electrospun fungal chitosan based nanofiber studies because the chitosan percentage yield from *R. oryzae* NRRL 1526 was higher than that of *A. niger* ATCC 16404. Different polymer solutions such as polyethylene oxide (PEO), polyvinyl alcohol (PVA), polycaprolactone (PCL), were used for most suitable fungal chitosan based electrospun nanofibers showed in Table 1. Solutions were stirred on a magnetic stirrer overnight to obtain homogenous polymer solution (Aliabadi et al., 2013; Dhandayuthapani et al., 2010; Levengood et al., 2017). The Ro-chitosan compared with commercial chitosan. PEO, PVA, PCL were dissolved in acetic acid, distilled water, trifluoroethanol (TFE), trifluoroacetic acid (TFA) solutions, respectively.

2.6 | Morphology and physicochemical properties of fungal chitosan based nanofiber

Characterization of electrospun Ro-chitosan based nanofiber that most suitable formula in Table 1 was carried out by SEM, FTIR, XRD (He et al., 2016; Yang et al., 2019). The morphology of the chitosan were analyzed by SEM. The samples were sputtercoated with gold for 30 s at 100 mA prior to imaging with a LEO 1430 VP SEM (Carl Zeiss AG, Jena, Germany) at an accelerating voltage of 20 kV. The diameter of the electrospun fibers was determined from SEM images.

FTIR spectra of nanofiber samples were examined by using a Perkin Elmer Spectrum Two spectrometer operated at 4 cm⁻¹ resolution. Each sample was pulverized and mixed with potassium bromide (KBr).

TABLE 1 Production of chitosan based nanofibers by electrospinning

Formula code	Concentration of polymer (w/v)	Electrospinning process parameters				
		Flow rate (ml/saat)	Voltage (kV)	Spinnerette-collector distance (mm)	Drum speed (rpm)	Oscillation range (mm)
F ₁	2% Ro-chitosan/EDTA (2:1) and 10% PVA (4:6) were prepared in distilled water	0.50	20	200	55	20
F ₂	2% Ro-chitosan/EDTA (2:1) and 10% PVA (3:7) were prepared in distilled water	0.25	20	200	55	20
F ₃	2% commercial chitosan /EDTA (2:1) and 12% PCL (3:7) were prepared in TFE	0.50	20	200	55	20
F ₄	2% Ro-chitosan/EDTA (2:1) and 12% PCL 3:7 were prepared in TFE	0.30	20	200	55	20
F ₅	2% commercial chitosan /EDTA (2:1) and 12% PCL (3:7) were prepared in TFE	0.30	20	200	55	20

The resultant suspension was pressed into a transparent pellet and examined in absorbance mode within the range of 400–4000 cm⁻¹.

The X-ray diffraction (XRD) patterns of nanofiber samples were acquired using a Bruker D8 Advance diffractometer (Cu K α radiation) operated at a scanning rate of 0.025°/s over a 2 θ range of 2°–60° and at 30 kV and 40 mA.

2.7 | Swelling test

Firstly, the dry weight of the nanofibers (W_d) were measured for determination of swelling (%) of Ro-chitosan based nanofiber and commercial chitosan based nanofiber. The nanofibers placed in the tubes that contains phosphate buffered saline (PBS, pH 7.4) and kept in a water bath at 37°C. At certain time intervals (0, 10, 20, 30, 40, 60, 80, 100, 120, 140, 180 and 220 min), the nanofiber samples were removed from the PBS, the excess water was removed with the help of filter paper and weighed again (W_w). Determination of the percent swelling of nanofiber was calculated according to the following equation (Ahamed & Sastry, 2011).

$$\%Swelling = [(W_w - W_d) / W_d] \times 100$$

3 | RESULTS

3.1 | Production of biomass and chitosan extraction

The biomass calculations of *A. niger* ATCC 16404 and *R. oryzae* NRRL 1526 were calculated as 5.4 g/L⁻¹ and 8.1 g/L⁻¹ after 6 days incubation in broth medium, respectively. Chitosan extraction was carried out by a modified method of Kleekayai and Suntornsuk (2010) from ground biomass. The percentage yield of Ro-chitosan and An-chitosan were determined as 18.6% and 12.5%, respectively.

3.2 | Characterization of fungal chitosan

The morphology and elemental composition of the Ro-chitosan, An-chitosan and commercial chitosan were analyzed by SEM and are shown in Figure 1. Also, EDX results of samples are shown in Table 2. It was observed that the Ro-chitosan, An-chitosan and commercial chitosan samples had a flat surface in some parts and a piecemeal surface in some parts and amorphous structure was observed as another important feature of the chitosan surface morphology. CK, OK, AuM, PdL elements were determined all chitosan samples. NaK, MgK were determined to Ro-chitosan, An-chitosan. Only PK were determined to An-chitosan.

The characterization of Ro-chitosan, An-chitosan and commercial chitosan were performed by FTIR (Figure 2). FTIR spectrum of Ro-chitosan showed 10 evident peaks as 3293 cm⁻¹, 2918 cm⁻¹, 1633 cm⁻¹, 1576 cm⁻¹ ve 1465 cm⁻¹, 1379 cm⁻¹, 1148 cm⁻¹, 1078 cm⁻¹, 1013 cm⁻¹, 551 cm⁻¹. These values of An-chitosan were determined as 3267 cm⁻¹, 2931 cm⁻¹, 1642 cm⁻¹, 1555 cm⁻¹ ve 1412 cm⁻¹, 1370 cm⁻¹, 1149 cm⁻¹, 1074 cm⁻¹, 1030 cm⁻¹, 557 cm⁻¹. Considering the spectrum of commercial chitosan are found to be 3982 cm⁻¹, 1185 cm⁻¹, 687 cm⁻¹. A wide absorption band in the range of 3200–3600 cm⁻¹ is demonstrated by O-H vibration tensional. The peaks around 2900, 1600, 1300 and 1100 cm⁻¹ in the chitosan FTIR spectrum are due to an aliphatic C-H, amide I (NH deformation–NHCOCH₃), amide II, amide III and C-O vibrational tensional bonds, respectively. In general, the presence of chitosan appears in the peaks between 3000 and 3500 cm⁻¹ (NH bond) and 1400–1650 cm⁻¹ (C=O bond) bands.

The deacetylation degree of chitosan has a great influence on many parameters, especially its solubility. Chitosan is obtained as a result of a certain degree of deacetylation of chitin (60% and above) (Vilchez et al., 2005). The percentage of deacetylation degree of Ro-chitosan and An-chitosan were determined as 68.34% and 50.33%, respectively. 100% deacetylation degree is rare in chitosan production.

DSC thermograms of Ro-chitosan, An-chitosan and commercial chitosan are shown in Figures 3–5. DSC thermogram of Ro-chitosan a wide endothermic peak was detected in the range of 76.05–122.94°C and a wide exothermic peak in the range of 264.70–301.82°C. Wide

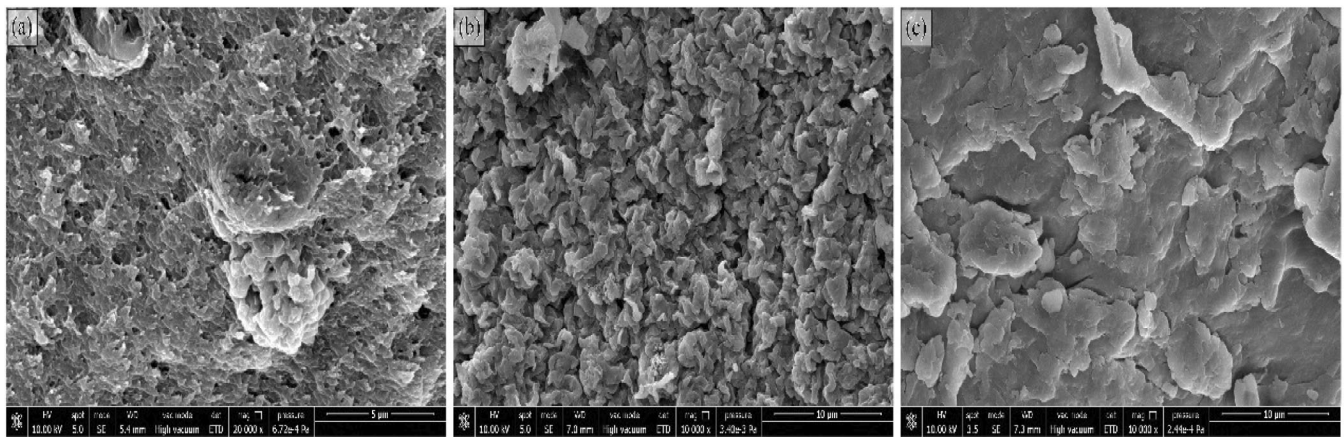


FIGURE 1 SEM images of Ro-chitosan (a), An-chitosan (b) and commercial chitosan (c).

TABLE 2 EDX results of fungal and commercial chitosan

Ro-chitosan			An-chitosan			Commercial chitosan		
Element	Weight%	Atomic%	Element	Weight%	Atomic%	Element	Weight%	Atomic%
CK	33.75	54.98	CK	45.58	71.98	CK	9.70	30.59
OK	26.07	31.36	OK	10.31	12.22	OK	15.74	37.26
NaK	1.31	1.10	NaK	4.75	3.92	NK	3.15	8.53
MgK	0.34	0.27	MgK	1.62	1.26	CIK	5.51	5.89
AuM	7.78	0.76	AuM	12.44	1.20	AuM	34.95	6.72
PdL	7.79	1.41	PdL	11.19	2.00	PdL	30.95	11.02
CaK	22.96	11.02	CaK	8.81	4.17			
			PK	5.30	3.25			

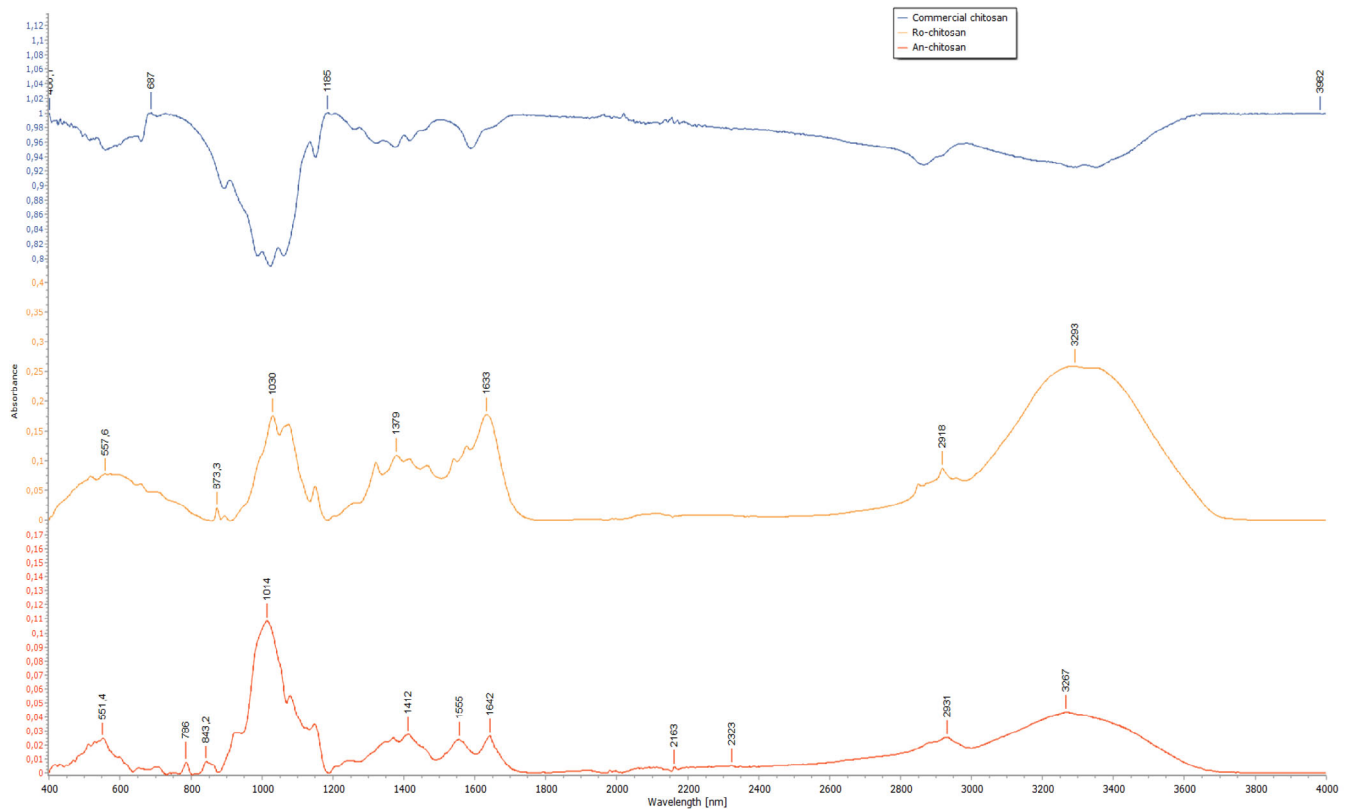


FIGURE 2 The FTIR spectrum of Ro-chitosan, An-chitosan and commercial chitosan.

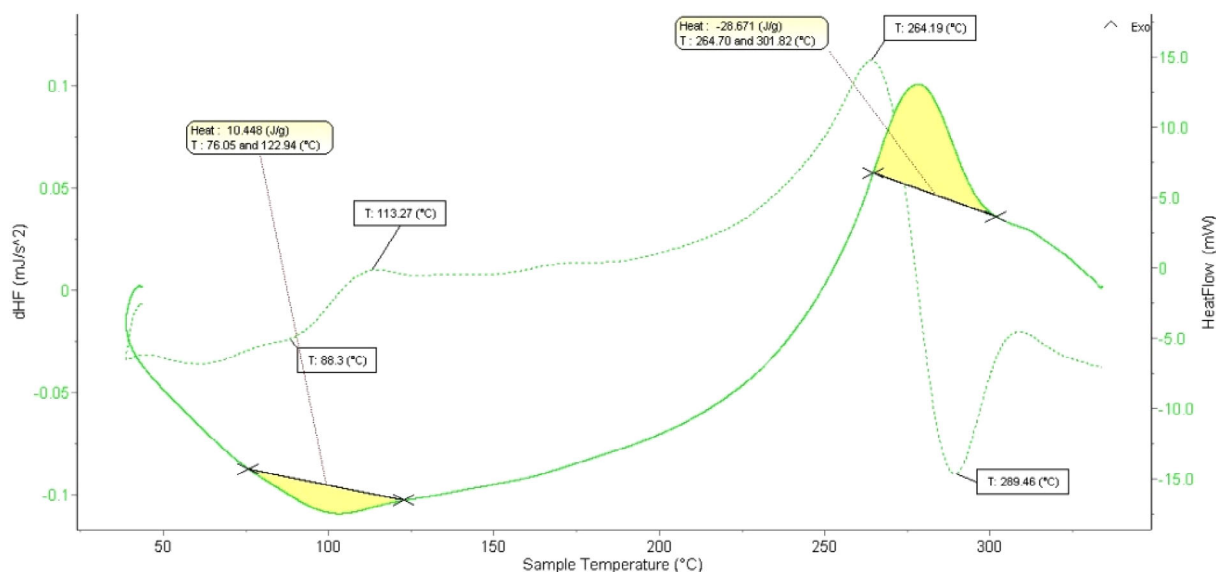


FIGURE 3 DSC thermogram of Ro-chitosan.

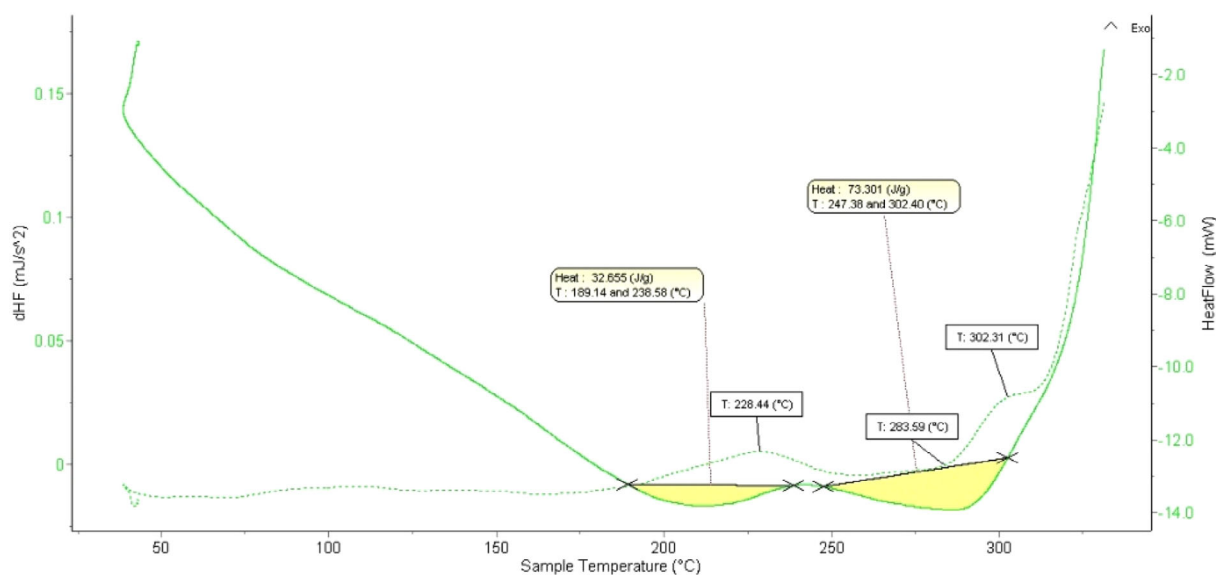


FIGURE 4 DSC thermogram of An-chitosan.

endothermic peaks were detected between 189.14–238.58 and 247.38–302.40°C in the DSC thermogram of An-chitosan. Wide endothermic peaks between 91.52–135.34 and 166.71–235.79 °C and an exothermic peak at 278.29–311.09°C were determined in the DSC thermogram of commercial chitosan.

3.3 | Cytotoxicity of fungal chitosan

Cytotoxicity of Ro-chitosan was determined by MTT assay on HDFa. The cell viability was higher than the control group at all concentrations for all time periods. All dose of sample showed

high cell viability and no cytotoxicity was observed (Figure 6). High cell viability was observed 375 µg/ml concentration at 24 and 48 h periods and 187.5 µg/ml concentration at the 72 h. If the concentration is above these concentrations, cell viability decreased compared to the control group.

3.4 | Morphology and physicochemical properties of electrospun chitosan based nanofibers

The images of the SEM analyzes of the electrospun nanofibers obtained from the formulations specified in Table 1 are shown in

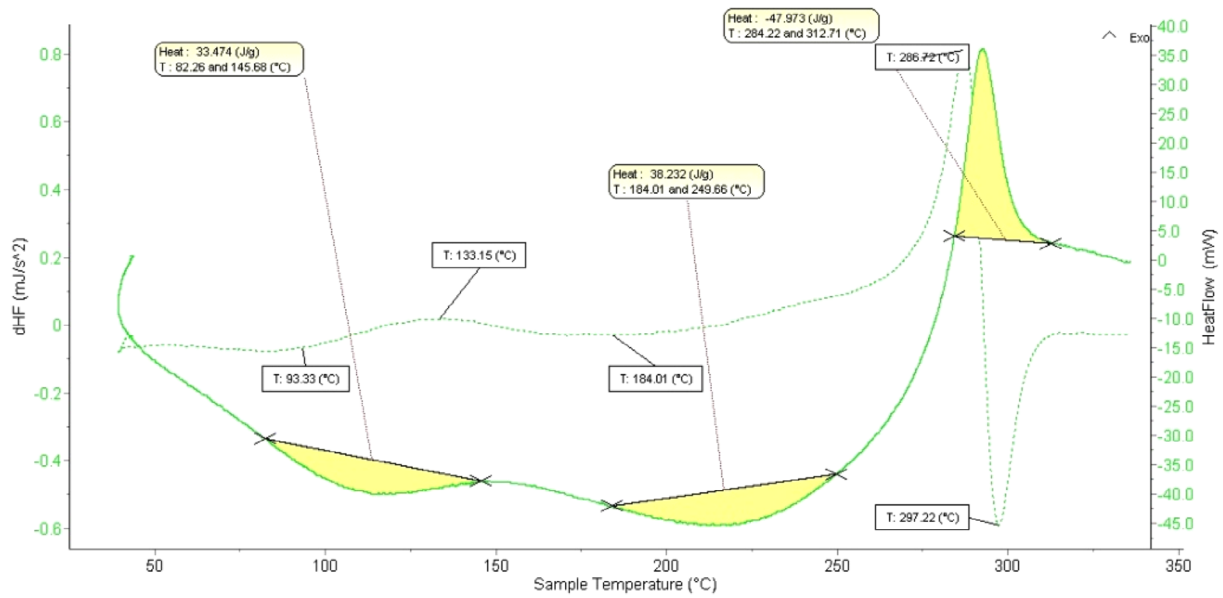


FIGURE 5 DSC thermogram of commercial chitosan. * $p < .005$, ** $p < .01$, *** $p < .001$, **** $p < .0001$.

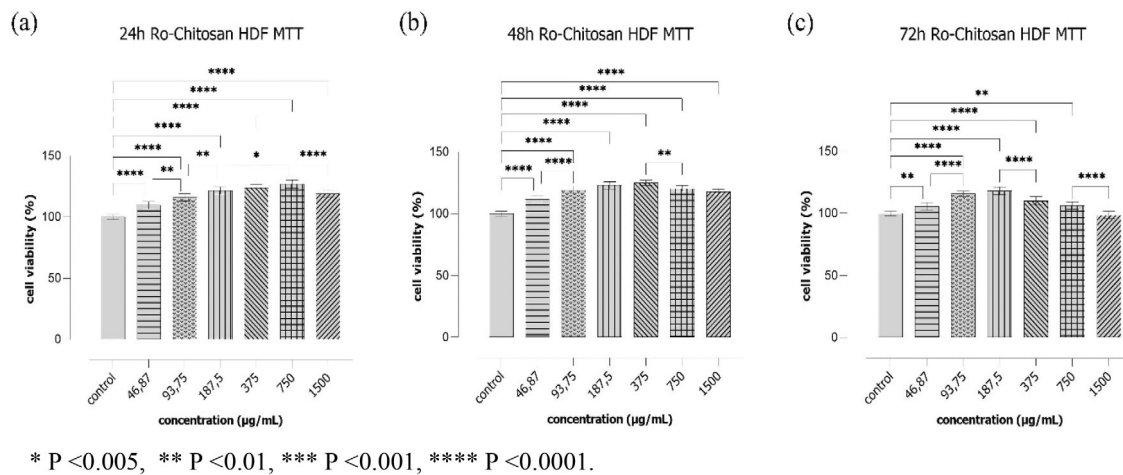


FIGURE 6 Cell viability of Ro-chitosan on HDFa cells for 24 (a), 48 (b), 72 h (c).

Figure 7. Among the electrospun formulas in Table 1, the F_4 formula which has the lowest average fiber diameter, the most uniform morphological structure and no beads structure were observed and F_4 formula was found more suitable than other formulas. Therefore, characterization studies were performed with F_4 formula and F_5 formula was used as a control. It has been determined that this F_4 and F_5 nanofiber structures were resistant to shrinkage, flexible and can be easily removed from the surface on which it is formed, without breaking down. Smooth nanofibers diameters determined to have an average fiber diameter of 100–120 nm. The nanofibers obtained from F_1 , F_2 , F_3 were evaluated as heterogeneous and irregular structures that contain large amounts of bead structures. The nanofibers obtained from F_4 and F_5 were

determined that the general homogeneous mesh appearance and very smooth and thin structure.

The nanofibers that obtained from F_3 , F_4 , F_5 formulas were removed from the surface on which it is formed but the other formulas were not removed on surface (Figure 8).

The FTIR spectrum of Ro-chitosan + PCL nanofiber (F_4) and commercial chitosan + PCL nanofiber (F_5) are shown in Figure 9. There were no significant differences determined between F_4 and F_5 nanofiber.

XRD is commonly used to determine the crystalline nature (Jana et al., 2014). XRD patterns of Ro-chitosan + PCL nanofiber is shown in Figure 10. According to test result there was significant weakening of characteristic peaks of PCL at 21.1° and 23.4° . Characteristic peaks

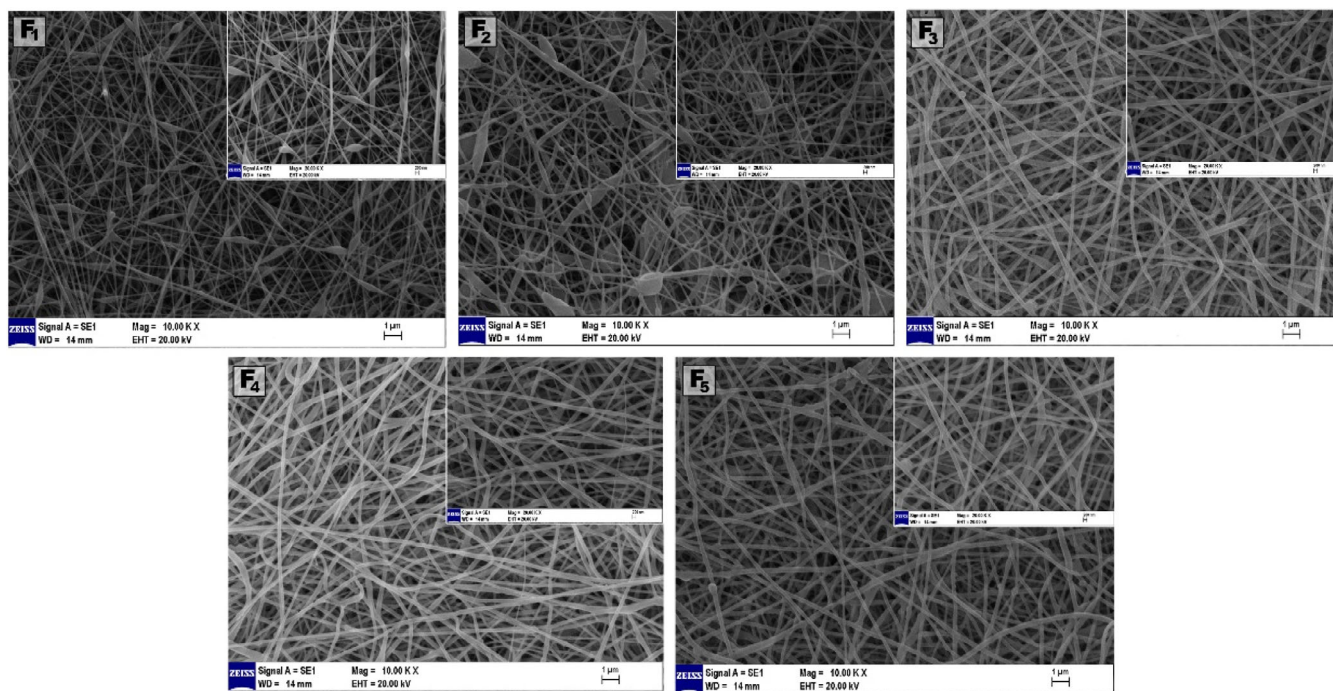


FIGURE 7 The images of the SEM analyzes of the electrospun nanofibers obtained from the formulations specified in Table 1.

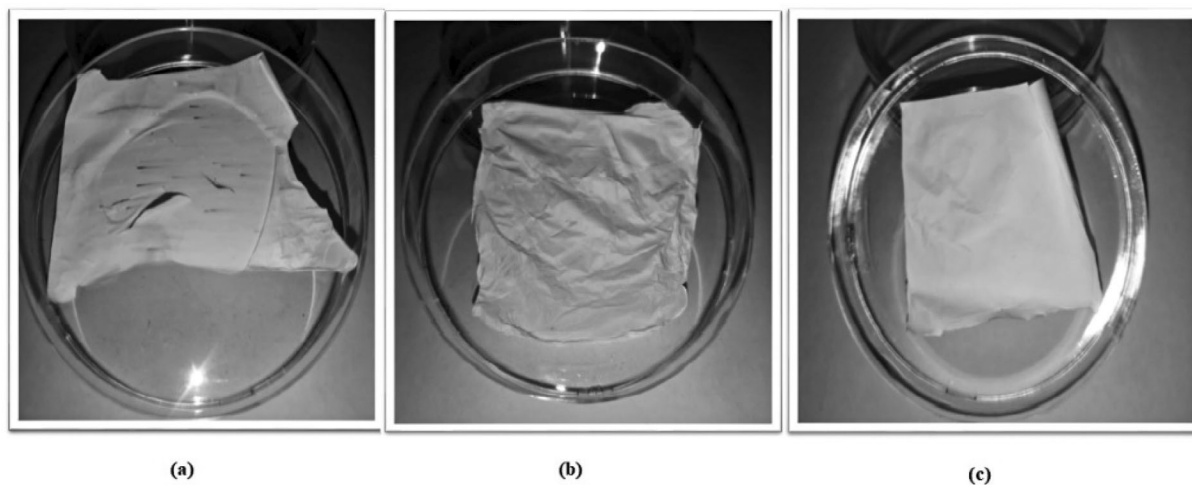


FIGURE 8 The nanofibers that obtained from F₃ (a), F₄ (b), F₅ (c) formulas.

of chitosan at 10.08° and 19.0° were seen in the Ro-chitosan + PCL spectrum. This is a clear indication for the formation of chitosan produced from *R. oryzae* NRRL 1526. The XRD pattern Ro-chitosan is shown in Figure 10.

Also in this study, nanofibers that obtained from F₄ and F₅ were analyzed for swelling percentage. % swelling rate of nanofibers were increased rapidly in the first hour then swelling rate of nanofibers increased more slowly and swelling rate fixed in 180–220 min. According to test results it was determined that Ro-chitosan + PCL nanofiber relatively higher swelling rates than PCL + commercial chitosan nanofiber (Figure 11).

4 | DISCUSSION

Chitin and chitosan are an integral part of the fungal cell wall of certain fungi. Several yeasts and fungal species have been previously investigated for chitosan production (Cardoso et al., 2012; Muslim et al., 2018). The chitosan obtained from fungal strains shows better uniformity in molecular weight, low polydispersity index and degree of deacetylation. Moreover, extraction of chitosan from fungal sources require less amount of chemicals as only mild conditions are needed for extraction and do not require stages, such as demineralization and depigmentation. Hence, producing a lower amount of toxic

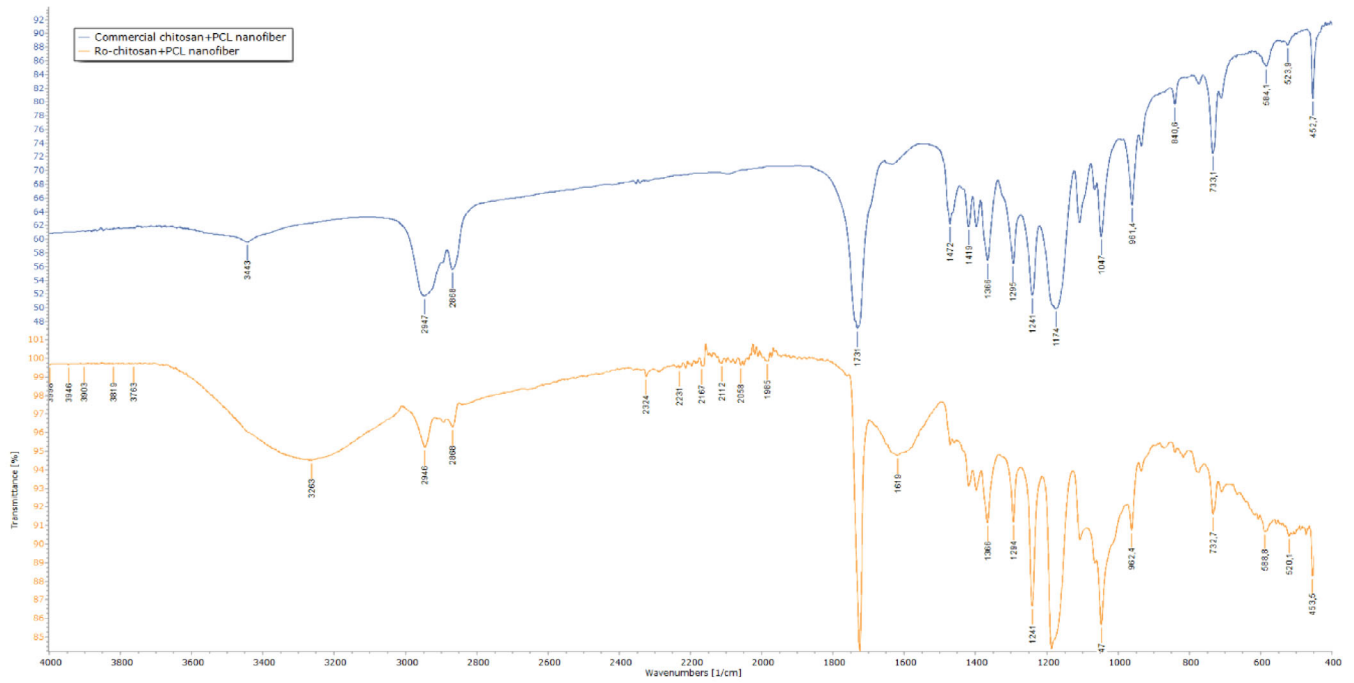


FIGURE 9 The FTIR spectrum of Ro-chitosan + PCL nanofiber and commercial chitosan + PCL nanofiber.

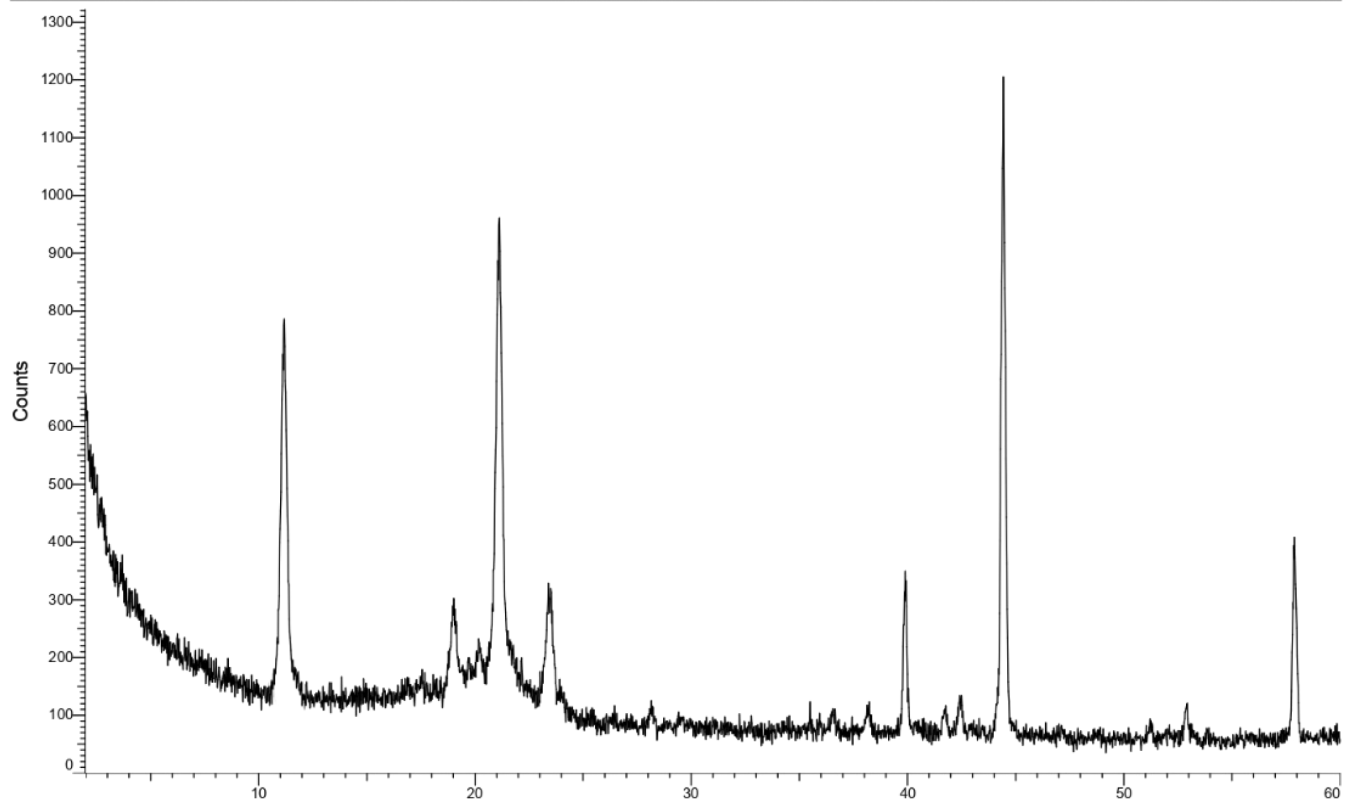


FIGURE 10 XRD spectra of Ro-chitosan + PCL nanofiber.

waste can be considered as a greener alternative. Pochanavanich and Suntornsuk (2002), evaluated the production and characterization of fungal chitosan (Pochanavanich & Suntornsuk, 2002). They showed

that *R. oryzae* TISTR3189 strain could produce high amount of chitosan. In another study, Cardoso et al. (2012) characterized by obtaining fungal chitosan from *R. arrhizus*. Gachhi and Hungun (2018) isolated

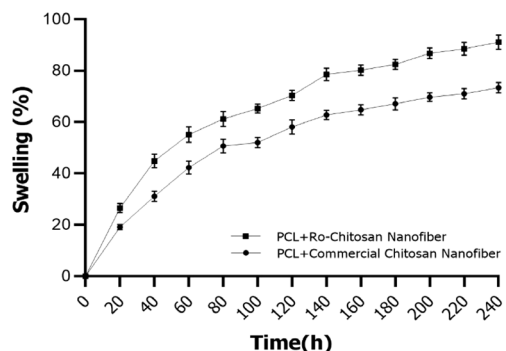


FIGURE 11 Swelling ratio (%) of nanofiber.

and characterized chitin-chitosan from *R. oryzae*. In present study, chitosan polymer was successfully obtained from *R. oryzae* NRRL 1526 and *A. niger* ATCC 16404 and characterization were carried out. The reason for choosing these species is that high chitosan production efficiency as a result of literature review (Abeer Mohammed, 2018; Sebastian et al., 2019). Abeer Mohammed (2018) investigated antimicrobial activity of chitosan that obtained from *A. niger* ATCC 16404 and percentage of chitosan yield was to be about 10%. In present study, the percentages of Ro-chitosan and An-chitosan were determined as 18.6% and 12.5%, respectively. In previous study Dhanashree et al. (2018) the maximum yield of chitosan (0.288 g/L) from *R. oryzae* NCIM 877 was obtained after 9 days of incubation. It is believed that the genetic singularity of the fungal species is responsible for the chitosan yield difference.

According to present results of SEM analyses, it was observed that fungal chitosan samples have amorphous structure. This is important feature of chitosan surface morphology. There are no significant differences determined between fungal chitosans and commercial chitosan.

Abeer Mohammed (2018) investigated the antimicrobial activity of chitosan that obtained from *A. niger*. As a result of the FTIR analysis of the chitosan six large peaks were determined. Among these peaks, the largest of them were determined as 3455.81 cm^{-1} and 1638.23 cm^{-1} wavenumbers. They stated that these peaks were associated with hydroxyl and amide groups. Other peaks were found as 2102.99 cm^{-1} , 1410.67 cm^{-1} , 1083.8 cm^{-1} and 546.72 cm^{-1} . The peak in the range of 1410.67 cm^{-1} indicated the presence of CH_3 methyl groups. This peak is associated with N-H deformation and indicates the degree of purity of chitosan. The literature for spectral analyses supports the infrared transmission spectral profile of extracted chitosan. Thus, the product is confirmed to be chitosan. Previous studies have showed that the percentage of N-acetyl glucosamine is higher in chitin and is lower in chitosan (Shelma & Sharma, 2011). The DD% is an important material and functional property of chitosan (Pochanavanich & Suntornsuk, 2002). In present study, deacetylation degree of Ro-chitosan and An-chitosan were determined as 68.34% and 50.33%, respectively. The results were slightly different from Pochanavanich and Suntornsuk (2002) reported that the percentages of chitosan yield and the deacetylation degree of chitosan obtained from *Rhizopus oryzae* TISTR3189 were determined as 14 and 87.9,

respectively. Similar to present study Dhanashree et al. (2018) the degree of deacetylation of chitosan from *Rhizopus oryzae* NCIM 877 were determined as 72.51.

DSC thermogram of Ro-chitosan revealed that it had a broad endothermic peak at $76.05\text{--}122.94^\circ\text{C}$ and a broad exothermic peak at $264.70\text{--}301.82^\circ\text{C}$. A wide endothermic peak at $90\text{--}100^\circ\text{C}$ was demonstrated that bound water molecules lost in sample. In addition, a sharp endothermic peak at 240°C showed that thermal degradation of sample (Ferrero & Periolatto, 2012; Shelma & Sharma, 2011). Also, exothermic peak at 300°C associated with the degradation of glucosamine (Orrego & Valencia, 2009).

According to percentage of chitosan yield and the results of characterization studies, Ro-chitosan was selected for subsequent studies. One drawback of pure chitosan as a biomaterial is its insufficient mechanical strength and lack of structural stability in aqueous environments due to swelling. Blending chitosan with the synthetic, biocompatible polymer, PCL, yields a copolymer blend with cell affinity, enhanced strength and stability as well as spinnability (Bhattaria et al., 2009; Jing et al., 2015; Prasad et al., 2015). In this study, Ro-chitosan based polymer solutions were prepared by adding different substances like as PVA, PCL and PEO to obtain electrospun nanofibers. According to SEM images the nanofiber structures were found to be beaded, non-beaded, smooth and non-uniform networks structures. For this reason, the most suitable nanofiber structure was obtained by using different electrostatic spinning parameters. Characterization studies of the most suitable nanofiber (F_4 formula) were carried out. Ro-chitosan + PCL nanofiber (F_4) was determined to be thin, bead-free, uniform fiber structure, flexible and easily remove from surface and taking the shape of the area. Thus, it was thought that it could be used as a wound dressing or a scaffold. PCL is a durable material gives it the ability to protect its form against external effects to the wound dressing being developed. Although clear data on the breaking strength and breaking elongation values of the nanofiber cannot be obtained, the fact that the nanofiber is not ruptured is an evidence that this is durable material. It is desired that the wound dressings have a high water holding capacity, as in our swelling test results showed that nanofibers with the desired properties could be obtained.

Dhanashree et al. (2018), characterization of chitin and chitosan from *R. oryzae* NCIM 877 were performed using FTIR and XRD methods. The prominent diffraction peak exhibited at $2\theta = 13$ and 20° are corresponding to the (020) and (110) plane of the semi-crystalline chitin and chitosan. This is a clear indication for the formation of chitin and chitosan produced from *R. oryzae*. In another study Jana et al. (2014) characterization of chitosan + PCL nanofiber was carried out by SEM, FTIR, XRD methods. According to XRD results there was significant weakening of characteristic peaks of PCL at 21.1° and 23.4° . Characteristic peaks of chitosan at 10.08° and 19.8° were seen in the chitosan + PCL spectrum. In present study, there are no significant changes observed between FTIR spectrums F_4 and F_5 nanofibers.

Chitosan is more hydrophilic than PCL, which is hydrophobic, whereas blending of these two polymers changes the swelling ratio of nanofibers. PCL is biocompatible and biodegradable polymer which

can be electrospun easily at low voltages and is able to provide required scaffold mechanical resistance. The mechanical properties of the scaffolds are related to the swelling of the scaffolds. Since the nanofiber wound dressing designed in this study is considered a wound contact layer, it was desired to have a high water-holding capacity (Jin et al., 2016). The high swelling ratio of the developed wound dressing model has desired properties for wound dressings. Also, the swelling is the sign that the body's immune system is working properly and repairing wound. F₄ nanofiber showed the relatively higher swelling compared to the F₅ nanofiber. The combination of PCL and chitosan polymers produced nanofiber structure that are hydrophilic, have high mechanical strength and longer degradation rates (Neves et al., 2011).

5 | CONCLUSIONS

In this study, chitosans were obtained from *Rhizopus oryzae* NRRL 1526 and *Aspergillus niger* ATCC 16404. According to percentage of chitosan yield and the results of the characterization studies, chitosan that obtained from *Rhizopus oryzae* NRRL 1526 was selected for subsequent studies. The results of characterization analysis of the fungal chitosan were revealed that the obtained biopolymer is actually chitosan and this polymer is usable for pharmaceutical areas and biotechnological applications. Also, the electrospun nanofiber that blends fungal chitosan and PCL polymers were fabricated successfully. The results of morphology and physicochemical properties of electrospun chitosan based nanofiber indicated that wound dressing models which combine the important intrinsic biological properties of chitosan and the mechanical integrity and stability of PCL were used as a potential wound dressings for tissue regeneration. The fungal chitosan/PCL nanofiber structures have significant potential in promoting tissue regeneration and physical properties of nanofibers such as fiber diameter, swelling rate, and surface area as well as scaffold porosity and stiffness.

AUTHOR CONTRIBUTIONS

Sevim Feyza Erdoğan: Conceptualization; investigation; writing – original draft; methodology; writing – review and editing; data curation; resources; software; project administration; formal analysis; visualization; validation. **Özlem Erdal Altıntaş:** Investigation; writing – review and editing; methodology; software; formal analysis; visualization. **Sefa ÇELİK:** Writing – review and editing; methodology.

FUNDING INFORMATION

This study was supported by a project of the Afyonkarahisar Health Sciences University Research Foundation, Project No. 19. TEMATİK.005.


CONFLICT OF INTEREST STATEMENT

On behalf of all authors, the corresponding author states that there is no conflict of interest.

DATA AVAILABILITY STATEMENT

The raw/processed data required to reproduce these findings are available from the corresponding author on reasonable request.

ORCID

Sevim Feyza Erdoğan  <https://orcid.org/0000-0002-4319-7558>
Özlem Erdal Altıntaş  <https://orcid.org/0000-0003-4680-1738>
Sefa ÇELİK  <https://orcid.org/0000-0002-5187-378X>

REFERENCES

- Abeer Mohammed, A. B. (2018). Production of chitosan from *aspergillus Niger* ATCC 16404 and application as antibacterial activity. *OBIMB*, 6(1), 48–50.
- Ahamed, M. I. N., & Sastry, T. P. (2011). Wound dressing application of chitosan based bioactive compounds. *International Journal of Pharmacy and Life Sciences*, 2(8), 991–996.
- Akila, R. M. (2014). Fermentative production of fungal chitosan, a versatile biopolymer (perspectives and its applications). *Advances in Applied Science Research*, 5(4), 157–170.
- Aliabadi, M., Irani, M., Ismaeili, J., Piri, H., & Parnian, M. J. (2013). Electrospun nanofiber membrane of PEO/chitosan for the adsorption of nickel, cadmium, lead and copper ions from aqueous solution. *The Chemical Engineering Journal*, 220, 237–243. <https://doi.org/10.1016/j.cej.2013.01.021>
- Bhattaria, N., Li, Z., Gunn, J., Leung, M., Cooper, A., Edmondson, D., Veisoh, O., Chen, M., Zhang, Y., Ellenbogen, R. C., & Zhang, M. (2009). Natural-synthetic polyblend nanofibers for biomedical applications. *Advanced Materials*, 21, 2792–2797. <https://doi.org/10.1002/adma.200802513>
- Bordes, P. E., & Averous, P. L. (2009). Nano-biocomposites: Biodegradable polyester/nanoclay systems. *Journal of Polity and Society*, 34, 125–155. <https://doi.org/10.1016/j.progpolymsci.2008.10.002>
- Cardoso, A., Lins, C. I. M., Santos, E. R., Silva, M. C. F., & Campos, T. G. M. (2012). Microbial enhance of chitosan production by *Rhizopus arrhizus* using agroindustrial substrates. *Molecules*, 17, 4904–4914. <https://doi.org/10.3390/molecules17054904>
- Chen, S., Liu, B., Carlson, M. A., Gombart, A. F., Reilly, D. A., & Xie, J. (2017). Recent advances in electrospun nanofibers for wound healing. *Nanomed*, 12(11), 1335–1352. <https://doi.org/10.2217/nnm-2017-0017>
- Dhanashree, B. G., & Hungund, B. S. (2018). Two-phase extraction, characterization, and biological evaluation of chitin and chitosan from *Rhizopus oryzae*. *Journal of Applied Pharmaceutical Science*, 8(11), 116–122.
- Dhandayuthapani, B., Krishnan, U. M., & Sethuraman, S. (2010). Fabrication and characterization of chitosan-gelatin blend nanofibers for skin tissue engineering. *Journal of Biomedical Materials Research-Part B: Applied Biomaterials*, 94(1), 264–272. <https://doi.org/10.1002/jbm.b.31651>
- Fathollahipour, S., Mehrizi, A. A., Ghaee, A., & Koosha, M. (2015). Electrospinning of PVA/chitosan nanocomposite nanofibers containing gelatin nanoparticles as a dual drug delivery system. *Journal of Biomedical Materials Research. Part A*, 103(12), 3852–3862. <https://doi.org/10.1002/jbm.a.35529>
- Ferrero, F., & Periolatto, M. (2012). Antimicrobial finish of textiles by chitosan uv-curing. *Journal of Nanoscience and Nanotechnology*, 12, 4803–4810. <https://doi.org/10.1166/jnn.2012.4902>
- Gachhi, D. B., & Hungun, B. S. (2018). Two-phase extraction, characterization, and biological evaluation of chitin and chitosan from *Rhizopus oryzae*. *Journal of Applied Pharmaceutical Science*, 8(11), 116–122. <https://doi.org/10.7324/JAPS.2018.81117>
- He, X., Li, K., Xing, R., Liu, S., Hu, L., & Li, P. (2016). The production of fully deacetylated chitosan by compression method. *Egyptian Journal of*

- Aquatic Research*, 42, 75–81. <https://doi.org/10.1016/j.ejar.2015.09.003>
- Huang, Z. M., Zhang, Y. Z., Kotaki, M., & Ramakrishna, S. (2003). A review on polymer nanofibers by electrospinning and their applications in nanocomposites. *Composites Science and Technology*, 63(15), 2223–2253. [https://doi.org/10.1016/S0266-3538\(03\)00178-7](https://doi.org/10.1016/S0266-3538(03)00178-7)
- Ifuku, S. (2014). (2014) chitin and chitosan nanofibers: Preparation and chemical modifications. *Molecules*, 19, 18367–18380. <https://doi.org/10.3390/molecules191118367>
- Jana, S., Leung, M., Chang, J., & Zhang, M. (2014). Effect of nano- and micro-scale topological features on alignment of muscle cells and commitment of myogenic differentiation. *Biofabrication*, 6, 35012. <https://doi.org/10.1088/1758-5082/6/3/035012>
- Jayakumar, R., Menon Manzoor, D. K., Nair, S. V., & Tamura, H. (2010). Biomedical applications of chitin and chitosan based nanomaterials—a short review. *Carbohydrate Polymers*, 82, 227–232. <https://doi.org/10.1016/j.carbpol.2010.04.074>
- Jin, S. G., Yousafa, A. M., Kima, K. S., Kima, D. W., Kima, D. S., Kima, J. K., Yongc, K. S., Yound, Y. S., Kimc, J. O., Choi, H. G., Jing, X., Mi, H. Y., Wang, X. C., Peng, X. F., & Turng, L. S. (2016). Influence of hydrophilic polymers on functional properties and wound healing efficacy of hydrocolloid based wound dressings. *International Journal of Pharmaceutics*, 501, 1–2. <https://doi.org/10.1016/j.ijpharm.2016.01.044>
- Jing, X., Mi, H.-Y., Wang, X.-C., Peng, X.-F., & Turng, L.-S. (2015). Shish-kebab-structured poly(ϵ -caprolactone) nanofibers hierarchically decorated with chitosan-poly(ϵ -caprolactone) copolymers for bone tissue engineering. *ACS Applied Materials & Interfaces*, 7, 6955–6965. <https://doi.org/10.1021/acsami.5b00900>
- Kamoun, E. A., & Kenawy, E. R. S. (2017). Chen X (2017) a review on polymeric hydrogel membranes for wound dressing applications: PVA-based hydrogel dressings. *Journal of Advanced Research*, 8(3), 217–233. <https://doi.org/10.1016/j.jare.2017.01.005>
- Kleekayai, T., & Suntornsuk, W. (2010). Production and characterization of chitosan obtained from *Rhizopus oryzae* grown on potato chip processing waste. *World Journal of Microbiology and Biotechnology*, 27, 1145–1154. <https://doi.org/10.1007/s11274-010-0561-x>
- Kucera, J. (2004). Fungal mycelium—the source of chitosan for chromatography. *Journal of Chromatography B*, 808(1), 69–73. <https://doi.org/10.1016/j.jchromb.2004.05.023>
- Kumar, P., Nagarajan, A., & Pradeep, D. U. (2018). Analysis of cell viability by the MTT assay. *Cold Spring Harbor Protocols*, 2018, pdb.prot095505. <https://doi.org/10.1101/pdb.prot095505>
- Kweon, H., Ha, H. C., Um, I. C., & Park, Y. H. (2001). Physical properties of silk fibroin/chitosan blend films. *Journal of Applied Polymer Science*, 80(7), 928–934.
- Levengood, S. L., Erickson, A. E., Chang, F., & Zhang, M. (2017). Chitosan-poly(caprolactone) nanofibers for skin repair. *Journal of Materials Chemistry. B, Materials for Biology and Medicine*, 5(9), 1822–1833.
- Li, J., He, A., Han, C. C., Fang, D., Hsiao, B. S., & Chu, B. (2006). Electrospinning of hyaluronic acid (HA) and HA/gelatin blends. *Macromolecular Rapid Communications*, 27(2), 114–120. <https://doi.org/10.1002/marc.200500726>
- Li, X., Shi, X., Wang, M., & Du, Y. (2011). Xylan chitosan conjugate: A potential food preservative. *Food Chemistry*, 126(2), 520–525. <https://doi.org/10.1016/j.foodchem.2010.11.037>
- Lin, H. Y., Chen, H. H., Chang, S. H., & Ni, T. S. (2013). Pectin-chitosan-PVA nanofibrous scaffold made by electrospinning and its potential use as a skin tissue scaffold. *Journal of Biomaterials Science. Polymer Edition*, 24(4), 470–481. <https://doi.org/10.1080/09205063.2012.693047>
- Majd, S. A., Khorasgani, M. R., Moshtaghian, S. J., Talebi, A., & Khezri, M. (2016). Application of chitosan/PVA Nano fiber as a potential wound dressing for streptozotocin-induced diabetic rats. *International Journal of Biological Macromolecules*, 92, 1162–1168. <https://doi.org/10.1016/j.ijbiomac.2016.06.035>
- Muslim, S. N., Al-Kadmy, I. M. S., Mohammed, A., Dwaish, A. N., Khazaal, A. S., & Aziz, S. N. (2018). Extraction of fungal chitosan and its advanced application. *Advanced Biotech*, 1, 1–17.
- Nemati, S., Kim, S. J., Shin, Y. M., & Shin, H. (2019). Current progress in application of polymeric nanofibers to tissue engineering. *Nano Convergence*, 6(1), 36. <https://doi.org/10.1186/s40580-019-0209-y>
- Neves, S. C., Teixeira, L. S. M., Moroni, L., Reis, R. L., Van Blitterswijk, C. A., Alves, N. M., Karperien, M., & Mano, J. F. (2011). Chitosan/poly(ϵ -caprolactone) blend scaffolds for cartilage repair. *Biomaterials*, 32(4), 1068–1079. <https://doi.org/10.1016/j.biomaterials.2010.09.073>
- No, H. K., Meyers, S. P., Prinyawiwatkul, W., & Xu, Z. (2007). Applications of chitosan for improvement of quality and shelf life of foods: A review. *Journal of Food Science*, 72, 87–100. <https://doi.org/10.1111/j.1750-3841.2007.00383.x>
- Nwe, N., Chandkrachang, S., Stevens, W. F., Maw, T., Tan, T. K., Khor, E., & Wong, S. M. (2002). Production of fungal chitosan by solid state and submerged fermentation. *Carbohydrate Polymers*, 49(2), 235–237. [https://doi.org/10.1016/S0144-8617\(01\)00355-1](https://doi.org/10.1016/S0144-8617(01)00355-1)
- Orrego, C. E., & Valencia, J. S. (2009). Preparation and characterization of chitosan membranes by using a combined freeze gelation and mild crosslinking method. *Bioprocess and Biosystems Engineering*, 32(2), 197–206. <https://doi.org/10.1007/s00449-008-0237-1>
- Pochanavanich, P., & Suntornsuk, W. (2002). Fungal chitosan production and its characterization. *Letters in Applied Microbiology*, 35, 17–21. <https://doi.org/10.1046/j.1472-765X.2002.01118.x>
- Prasad, T., Shabeena, E. A., Vinod, D., Kumary, T. V., & Anil Kumar, P. R. (2015). Characterization and in vitro evaluation of electrospun chitosan/polycaprolactone blend fibrous mat for skin tissue engineering. *Journal of Materials Science. Materials in Medicine*, 26, 5352. <https://doi.org/10.1007/s10856-014-5352-8>
- Ramakrishna, S., Fujihara, K., Teo, W. E., Lim, T. C., & Ma, Z. (2005). An introduction to electrospinning and nanofibers. *Electrospin Nonofiber*, 90–154. <https://doi.org/10.1142/5894>
- Schiffman, J. D., & Schauer, C. L. (2007). One-step electrospinning of cross-linked chitosan fibers. *Biomacromolecules*, 8, 2665–2667. <https://doi.org/10.1021/bm7006983>
- Sebastian, J., Rouissi, T., Brar, K. S., Hedge, K., & Verma, M. (2019). Microwave-assisted extraction of chitosan from *Rhizopus oryzae* NRRL1526 biomass. *Carbohydrate Polymers*, 219, 431–440. <https://doi.org/10.1016/j.carbpol.2019.05.047>
- Shao, W., He, J., Sang, F., Wang, Q., Chen, L., Cui, S., & Ding, B. (2016). Enhanced bone formation in electrospun poly(l-lactic-co-glycolic acid)-tussah silk fibroin ultrafine nanofiber scaffolds incorporated with graphene oxide. *Materials Science and Engineering: C*, 62, 823–834. <https://doi.org/10.1016/j.msec.2016.01.078>
- Shelma, R., & Sharma, C. P. (2011). Development of lauroyl sulfated chitosan for enhancing hemocompatibility of chitosan. *Colloids and Surfaces B*, 84(2), 561–570. <https://doi.org/10.1016/j.colsurfb.2011.02.018>
- Subbiah, T., Bhat, G. S., Tock, R. W., Parameswaran, S., & Ramkumar, S. S. (2005). Electrospinning of nanofibers. *Journal of Applied Polymer Science*, 96, 557–569. <https://doi.org/10.1021/acs.chemrev.8b00593>
- Tajdini, F., Amini, M. A., Nafissi-Varcheh, N., & Faramarzi, M. A. (2010). Production, physicochemical and antimicrobial properties of fungal chitosan from *Rhizomucor miehei* and *Mucor racemosus*. *International Journal of Biological Macromolecules*, 47(2), 180–183. <https://doi.org/10.1016/j.ijbiomac.2010.05.002>
- Tripatanasuwan, S., Zhong, Z., & Reneker, D. H. (2007). Effect of evaporation and solidification of the charged jet in electrospinning of poly(ethylene oxide) aqueous solution. *Polymer*, 48(19), 5742–5746. <https://doi.org/10.1016/j.polymer.2007.07.045>
- Tucker, N., Stanger, J. J., Staiger, M. P., Razaq, H., & Hofman, K. (2012). The history of the science and technology of electrospinning from 1600 to 1995. *Journal of Engineered Fibers and Fabrics*, 1, 63–73. <https://doi.org/10.1177/155892501200702510>

- Venugopal, J., Prabhakaran, M. P., Zhang, Y. Z., Low, S., Choon, A. T., & Ramakrishna, S. (2010). Biomimetic hydroxyapatite-containing composite nanofibrous substrates for bone tissue engineering. *Philosophical Transactions of the Royal Society*, 368, 2065–2081. <https://doi.org/10.1098/rsta.2010.0012>
- Vilchez, S., Jovancic, P., Manich, A. M., Julia, M. R., & Erra, P. (2005). Chitosan application on wool before enzymatic treatment. *Journal of Applied Polymer Science*, 98, 1938–1946.
- Wu, T., Zivanovic, S., Draughon, F. A., Conway, W. S., & Sams, C. E. (2005). Physicochemical properties and bioactivity of fungal chitin and chitosan. *Journal of Agricultural and Food Chemistry*, 53, 3888–3894. <https://doi.org/10.1021/jf048202s>
- Yang, S., Zhang, X., & Zhang, D. (2019). Electrospun chitosan/poly (vinyl alcohol)/graphene oxide nanofibrous membrane with ciprofloxacin

antibiotic drug for potential wound dressing application. *International Journal of Molecular Sciences*, 20(18), 4395–4411. <https://doi.org/10.3390/ijms20184395>

How to cite this article: Erdoğan, S. F., Altıntaş, Ö. E., & ÇELİK, S. (2023). Production of fungal chitosan and fabrication of fungal chitosan/polycaprolactone electrospun nanofibers for tissue engineering. *Microscopy Research and Technique*, 1–13. <https://doi.org/10.1002/jemt.24315>